

# Few-Shot Font Generation by Learning Fine-Grained Local Styles

Licheng Tang<sup>1\*</sup> Yiyang Cai<sup>2\*</sup> Jiaming Liu<sup>1†</sup> Zhibin Hong<sup>1</sup> Mingming Gong<sup>3</sup>  
 Minhu Fan<sup>1</sup> Junyu Han<sup>1</sup> Jingtuo Liu<sup>1</sup> Errui Ding<sup>1</sup> Jingdong Wang<sup>1</sup>  
<sup>1</sup>Baidu Inc. <sup>2</sup>University of California, Berkeley <sup>3</sup>University of Melbourne

{tanglicheng, liujiaming03, hongzhibin, fanminhu, liujingtuo, dingerrui, wangjingdong}@baidu.com  
 frank.cai@berkeley.edu, mingming.gong@unimelb.edu.au

## Abstract

Few-shot font generation (FFG), which aims to generate a new font with a few examples, is gaining increasing attention due to the significant reduction in labor cost. A typical FFG pipeline considers characters in a standard font library as content glyphs and transfers them to a new target font by extracting style information from the reference glyphs. Most existing solutions explicitly disentangle content and style of reference glyphs globally or component-wisely. However, the style of glyphs mainly lies in the local details, i.e. the styles of radicals, components, and strokes together depict the style of a glyph. Therefore, even a single character can contain different styles distributed over spatial locations. In this paper, we propose a new font generation approach by learning 1) the fine-grained local styles from references, and 2) the spatial correspondence between the content and reference glyphs. Therefore, each spatial location in the content glyph can be assigned with the right fine-grained style. To this end, we adopt cross-attention over the representation of the content glyphs as the queries and the representations of the reference glyphs as the keys and values. Instead of explicitly disentangling global or component-wise modeling, the cross-attention mechanism can attend to the right local styles in the reference glyphs and aggregate the reference styles into a fine-grained style representation for the given content glyphs. The experiments show that the proposed method outperforms the state-of-the-art methods in FFG. In particular, the user studies also demonstrate the style consistency of our approach significantly outperforms previous methods.

## 1. Introduction

In the modern era, both computer systems and humans process huge amounts of text information. Fonts, the representations of text, have thus played critical roles in many

\*Equal contribution.

†Corresponding author.

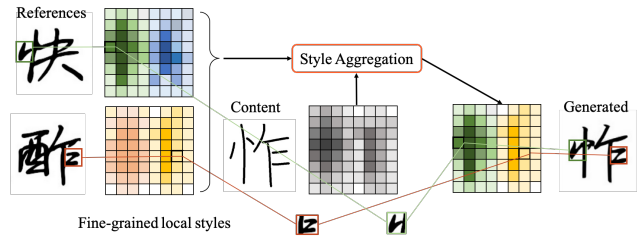


Figure 1. Our proposed fine-grained local style extraction and style aggregation process. Our proposed module enables fine-grained style extraction from references and learns the correspondence between content and reference, thus aggregate corresponding local styles into correct locations in content with high-fidelity.

applications. Therefore, the stylish font generation has its unique commercial and artistic values. However, building commercial font libraries is costly and labor-intensive. The cost is even higher for those languages with a huge amount of characters (Chinese, Japanese Kanji, Korean, Thai, etc.).

Due to the expert’s high cost of building fonts, automatic font generation with deep learning has drawn rising attention. It aims at generating a brand new font library with only a few characters as a reference. With the development of Generative Adversarial Networks (GANs) [10, 20], there have been many classic works of font generation. Early attempts, such as zi2zi [26], use Pix2Pix [14] like networks with a plug-in font category embedding conditions to learn multiple font styles with a single model. However, these methods require a large number of glyphs to train each unseen font.

In recent years, some works tried to tackle few-shot font generation (FFG) with a few-shot Image-to-Image translation (I2I) scheme [4, 8, 22, 23, 31]. Unlike zi2zi, the font style representation is learned from a few reference exemplars, rather than learning embeddings from different font labels. One popular strategy of these works is to explicitly disentangle the content and style representations from given content images and reference exemplars, and two representations are then combined and decoded into the target glyphs. With the advance of these works, the generated glyphs’

quality is significantly improved when the number of references is limited. Based on the explicit disentanglement ideas, the research of FFG can be divided into two different categories, i.e. global style representation and component-wise style representation. The former one models the glyph style as universal representation for each font [8, 18, 31], while the latter one utilizes component-wise style representation from different reference exemplars in the same font [4, 13, 22, 23].

However, in a commercial font, multiple levels of styles need to be considered. An expert would carefully design every possible detail. The detailed styles among components, strokes and, even edges are designed to be consistent. Previous works mostly focus on component-wise styles, while largely ignoring the finer-grained styles. Meanwhile, since the content and style are highly entangled, the commonly used explicit disentanglement can hardly assure the consistency of component-wise styles between the reference glyphs and the generated glyphs. To this end, we employ a references encoder to learn the fine-grained local styles (*FLS*) without explicit disentangled representation learning. Instead of regarding the overall reference map as style, we consider each spatial location of the feature map as a *FLS* representation of reference glyph. After learning the spatial correspondence between references and content, we further acquire the target style map by aggregating the corresponding *FLS*s from references. Each feature vector of the target style map also represents *FLS*s for the target glyph.

In this paper, we propose a novel approach shown in Figure 1, named FSFont for few-shot font generation. The reference glyph images are encoded into reference maps, which represent the *FLS*s of the references. Our proposed cross-attention based style aggregation module (SAM) learns the spatial correspondence between references and the content glyph. The spatial correspondence is not only on the component level but also on the granular level, which contains more detailed local styles. Afterward, SAM aggregates the *FLS*s of references into the target style map, where each spatial location can be assigned to the right fine-grained style. Moreover, to enhance the model to recover details of the references better and learn correspondence more effectively, we adapt a self-reconstruction branch that takes the target character as the input of the reference encoder, and the generated result is supervised by itself. This branch makes learning the correspondence more easily, and helps to produce highly consistent output. Last but not least, we develop a strategy to select the references for each glyph automatically. After analyzing the compositional rules, we design a breadth-first search-based algorithm to search for the reference set and find the optimal references for each character.

In summary, the contribution of this paper is threefold:

- We devise a novel model for few-shot generation. The

model extracts the *FLS* of the reference glyph images, and a cross-attention based style aggregation module aggregates the reference styles into a target style map. The details from reference glyphs are thereby transferred to the target glyph.

- We propose a unified training framework with a newly designed self-reconstruction branch. This branch significantly boosts the detail capture ability of the model and improves the output images' quality. As a result, the proposed full model achieves state-of-the-art font generation results.
- We analyze the relationship between characters and select a fairly small set of characters as references. Then we develop a rule to map each character with the elements in the reference set. With the proposed rule, the model's ability to extract component features is better exploited.

## 2. Related Works

### 2.1. Image-to-image translation

Image-to-image (I2I) translation refers to the task of learning a mapping function between the source domain and target domain, which preserves the content of the source image while merging the style of the target domain at the same time. According to many I2I methods [6, 7, 14, 17, 18, 32, 34], I2I methods have developed towards multi-mapping [7, 17, 32] and few-shot learning [18]. CycleGAN [34] introduces the cycle-consistency into generative models, which enables I2I methods to train cross-domain translation without paired data. FUNIT [18] accomplish the style transfer task by encoding content and style respectively and combine them with adaptive instance normalization (AdaIN) [12]. From an intuitive thought, font generation is a typical I2I translation task, since it tries to keep the content information of the source font and maps it into the target font. Thus, many font generation methods are based on I2I translation methods.

### 2.2. Many-shot font generation

Early font generation methods [5, 9, 11, 15, 16, 19, 24–26, 28, 30] aim at learning a mapping function between source fonts and target fonts. When new font references are introduced, these methods use hundreds of reference glyphs to fine-tune the original mapping function. zi2zi [26] and Rewrite [25] train GANs in a supervised way with one-hot style labels. AGEN [19] proposes an model based on the auto encoder to transfer standard font images to calligraphy images. HAN [5] designs skip connection and hierarchical loss functions to improve zi2zi's generation performance.

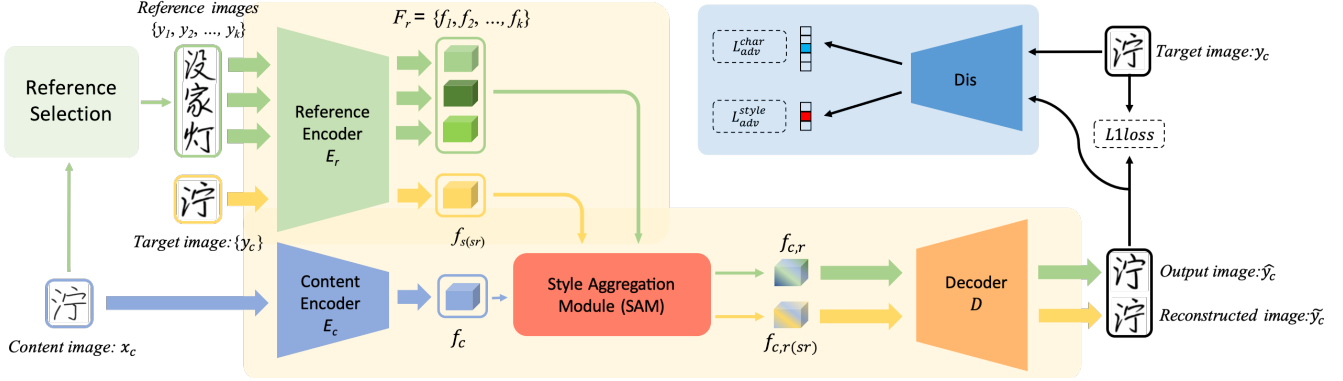


Figure 2. **Overview of our proposed model.** Our generator consists of four parts: a reference encoder  $E_r$ , a content encoder  $E_c$ , the **Style Aggregation Module (SAM)**, and a decoder  $D$ . Given a content image  $x_c$  and  $k$ -shot references  $\{y_1, y_2, \dots, y_k\}$  which is selected based on our proposed **Reference Selection**,  $E_r$  and  $E_c$  extract their features  $F_r$  and  $f_c$  respectively. Our SAM matches  $F_r$  and  $f_c$  based on the attention mechanism and links them with spatial correspondence, outputting the target style map  $f_{c,r}$ . Afterwards, we use  $D$  to obtain the generated image  $\hat{y}_c$ . We also propose a auxiliary branch of **Self-Reconstruction** during training stage (yellow branch). It shares weights with the main branch and improves generated images' quality in details. A multi-task discriminator is employed to calculate the adversarial loss and simultaneously distinguish the content and style category of the generated character. We also compute the pixel-wise reconstruction loss between the ground truth  $y_c$  and the generated image  $\hat{y}_c$ , and between  $y_c$  and the reconstructed image  $\tilde{y}_c$ , respectively.

These methods require paired data to train a mapping function, e.g., 775 for [16]. Other methods [9, 11] focus on unpaired data, and use them for style extraction. Although these many-shot font generation methods have achieved remarkable performance, it is still a laborious task to collect hundreds of references for the fine-tuning process, especially when the reference font library is glyph-rich.

### 2.3. Few-shot font generation

Most Few-shot font generation (FFG) methods focus on disentangling the content feature and style feature from the given glyphs. Based on different kinds of feature representation, FFG methods can be divided into two main categories: global feature representation [1, 8, 29, 33] and component-based feature representation [4, 13, 22, 23]. In methods that apply global feature representation, vectors related to content and style are extracted from content glyphs and reference glyphs respectively. MCGAN [1] synthesizes the ornamented glyphs with stacked conditional GANs to extract features from input images. EMD [33] and AGIS-Net [8] combine a style vector and content vector together to synthesize a glyph. ZiGAN [29] matches the features to Hilbert space to better capture the structural information. Works related to component-based feature representation concentrate on devising a feature representation that is related to the glyphs' components or localized features. RD-GAN [13] uses a radical encoder to extract features of glyphs' specific components. In DM-Font [4], it disassembles glyphs to stylized components and reassembles them to new glyphs by utilizing strong compositionality prior. LF-Font [22] designs a component-conditioned reference encoder to extract component-wise features from reference

images. MX-Font [23] employs multiple encoders for each reference image with disentanglement between content and style which makes the cross-lingual task possible. DG-Font [31] is an unsupervised framework based on TUNIT [2] by replacing the traditional convolutional blocks with Deformable blocks which enables the model to perform better on cursive characters which are more difficult to generate.

However, the previous FFG works fail to fully explore the style maps from  $k$ -shot references. When receiving  $k$ -shot reference images, they tend to explicitly disentangle *style* and *content* of images globally or component-wisely and conduct an average operation among extracted features [22, 23]. The local details extracted from each reference are significantly weakened by disentanglement and the average operation. Therefore, we design *Style Aggregation Module* that aims to keep the very detailed features from reference images and to fully utilize the spatial details.

### 2.4. Attention Mechanism

The attention mechanism [27] is known to capture dependence. After its debut in machine translation, it has been applied in many vision tasks including font generation. RD-GAN [13] uses attention mechanism to extract rough radicals from content characters and then render them into target style. HWT [3] uses transformer blocks to bridge the gap between image and text, making it capable of generating stylized handwriting English text images. Our *Style Aggregation Module* is highly motivated by the attention mechanism for fine-grained feature map re-composition.

### 3. Method

In this section, we present the details of our FS-Font method. We first briefly review the few-shot font generation problem setup and introduce the overall framework of our method (3.1). Next, we present the details of three crucial components of our approach, including the *Style Aggregation Module* (SAM) (Sec. 3.2), the Self-Reconstruction branch (Sec. 3.3), and Reference Selection (Sec. 3.4).

#### 3.1. Problem Setting and Method Overview

In few-shot font generation, given a content glyph image  $x_c$  with the content  $c$  from a standard font  $X = \{x_c\}_{c=1}^N$  and a  $k$ -shot reference glyph images with the style  $s$ :  $R_s = \{y_i\}_{i=1}^k \subset Y_s$ , our goal is to generate a stylized image  $\hat{y}_c$  that has the content  $c$  and style  $s$  via a generator  $G$ :

$$\hat{y}_c = G(x_c, R_s), \quad (1)$$

where the style  $s$  of  $\hat{y}_c$  is omitted for sake of simplicity.

In training, we collect  $L$  fonts with different styles  $Y = \{Y_s\}_{s=1}^L$ , where  $Y_s = \{y_c\}_{c=1}^N$ . Therefore, we have a paired dataset  $\{x_c, y_c\}_{c=1}^N$  for each content  $c$  in  $s$ -th training style.

The overall framework is shown in Figure 2. The reference encoder  $E_r$  first encodes  $R_s$  into  $k$ -shot reference maps  $F_r = \{f_i\}_{i=1}^k$ , where  $f_i$  is encoded from  $y_i$ . The content encoder  $E_c$  extracts the content feature map  $f_c$  from the input content image  $x_c$ . Our proposed SAM takes  $F_r$  and  $f_c$  as inputs, attends to the corresponding spatially local styles in the reference maps  $F_r$  and aggregates the local styles into the target style map  $f_{c,r} = SAM(f_c, F_r)$ . In the end, the decoder  $D$  decodes  $f_{c,r}$  into the generated output image  $\hat{y}_c$ . A multi-task projection discriminator [21] is employed to discriminate each generated image and real image. The discriminator outputs a binary classification of fake or real for each character’s style and content category.

#### 3.2. Style Aggregation Module

An overview of the SAM is depicted in Figure 3. The core in SAM is a multi-head cross attention block that attends to spatially local styles from the reference maps  $F_r$  and aggregates the reference styles into the fine-grained style representation for the given content image. For the  $m$ -th attention head, SAM learns a Query map  $Q^m$  from content feature map  $f_c$  and Key map  $K^m$  from reference maps  $F_r$ , which achieves the spatial correspondence matrix  $A^m$  between the pixels of  $Q^m$  and  $K^m$ . A value map  $V^m$  is simultaneously learned from  $F_r$ . Multiplying the correspondence matrix  $A^m$  with the value map  $V^m$  aggregates the local style styles into the target style  $S^m$ . As different head captures different information, we combine all the target styles together for decoding.

Formally, we reshape  $f_c \in \mathbb{R}^{c \times h \times w}$  into a sequence  $\tilde{f}_c \in \mathbb{R}^{c \times (h \cdot w)}$ , where  $(h, w)$  is the resolution of the feature

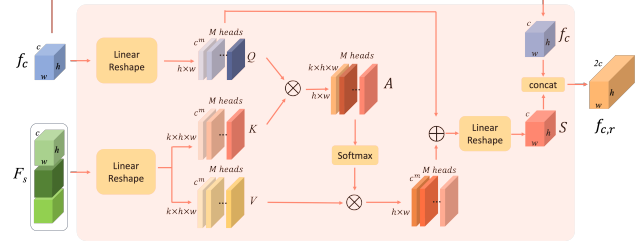


Figure 3. **The illustration of the Style Aggregation Module (SAM).** We use multihead attention mechanism to calculate the spatial correspondence of content and references and generate the fine-grained feature map.

map,  $c$  is the number of channels. For the  $m$ -th head, after applying a linear layer  $L_{query}^m \in \mathbb{R}^{c \times c^m}$ , we acquire the query matrix  $Q^m \in \mathbb{R}^{c^m \times (h \cdot w)}$ . Meanwhile, the reference maps  $F_r = \{f_i\}_{i=1}^k$  are reshaped and concatenated along the spatial dimension  $(h, w)$ , forming a reference sequence  $\tilde{f}_r \in \mathbb{R}^{c \times (k \cdot h \cdot w)}$ . We multiply  $\tilde{f}_r$  by two linear projections  $L_{key}^m, L_{value}^m \in \mathbb{R}^{c \times c^m}$  and generate a key map  $K^m$  and a value map  $V^m$  as follows:

$$\begin{aligned} Q^m &= L_{query}^m(\tilde{f}_c), & Q^m &\in \mathbb{R}^{c^m \times (h \cdot w)}, \\ K^m &= L_{key}^m(\tilde{f}_r), & K^m &\in \mathbb{R}^{c^m \times (k \cdot h \cdot w)}, \\ V^m &= L_{value}^m(\tilde{f}_r), & V^m &\in \mathbb{R}^{c^m \times (k \cdot h \cdot w)}. \end{aligned} \quad (2)$$

We then compute a spatial correspondence matrix  $A^m$  of which each element  $A^m(u, v)$  is a pairwise feature correlation between content feature in position  $u$  and reference feature in position  $v$ , calculated as follows:

$$A^m = \frac{Q^{m\top} K^m}{\sqrt{c^m}} \in \mathbb{R}^{h \times w \times k \cdot h \cdot w}, \quad (3)$$

where  $c^m$  is the hidden dimension of  $Q^m$  and  $K^m$ . The  $1/\sqrt{c^m}$  factor follows Transformers [27] to prevent the magnitude of the dot product from growing extreme.

With the correspondence matrix  $A^m$ , we obtain the aggregated style from references by

$$S^m = softmax(A^m) V^{m\top} \in \mathbb{R}^{h \times w \times c^m}. \quad (4)$$

After permuting and reshaping  $S^m$  into  $\mathbb{R}^{c^m \times h \times w}$ , we concatenate all  $S^m$  along the channel dimension, and employ a linear projection  $L_s \in \mathbb{R}^{(c^m \cdot M) \times c}$  to obtain  $S$ . The target style map  $f_{c,r}$  is obtained as the concatenation between  $S$  and content feature  $f_c$ . The decoder  $D$  decodes it into the target image  $\hat{y}_c$  as follows:

$$\begin{aligned} S &= L_s(S^1 \circ S^2, \dots, \circ S^M) \in \mathbb{R}^{c \times h \times w}, \\ \hat{y}_c &= D(f_{c,r}) = D(f_c \circ S), \end{aligned} \quad (5)$$

where  $\circ$  denotes concatenation operator and  $M$  is the number of total attention heads.

### 3.3. Self Reconstruction

To achieve a highly style-consistent glyph using SAM, it depends not only on the proper aggregation of styles, but also on the expressivity of the styles that depict fine and local details of the references. However, the  $k$ -shot font generation setup is a hard-to-learn problem, as it requires the attention learns spatial correspondence from weakly correlated content-references pairs, which is sometimes confusing even for a human expert. Thus, besides the main branch of  $k$ -shot learning, we introduce an easy-to-learn Self-Reconstruction (SR) branch to boost the learning process.

While the generator is trained in the above mentioned  $k$ -shot setup, for a given content input  $x_c$ , we have the ground truth image  $y_c$  to supervise the model training. Self Reconstruction is a parallel branch that shares the same model as the main branch during training. It takes  $y_c$  as the reference image  $\tilde{R}_s = \{y_c\}$ , and its output  $\tilde{y}_c$  is also supervised by  $y_c$  itself. In contrast to Eq. 1, the generation process of this branch is

$$\tilde{y}_c = G(x_c, \tilde{R}_s). \quad (6)$$

The detailed training setup can be found in Sec.3.5. In the SR branch, the content and reference images are strongly correlated. The spatial correspondence matrix can be easily learned as the strokes and the components' relationship between content and reference is clear. With the well-learned correspondence, the generator can be optimized with well-aligned gradients. As a result, the expressivity of depicting details can be further learned within our framework.

### 3.4. Reference Selection

In previous works considering the decomposition of components like LF-Font [22], reference characters that contain the same components as content character are randomly selected from the training set during each iteration. The model can hardly learn how to extract the right component-wise features with varying combinations of the reference set. Thus, we introduce a strategy to select a fixed reference set whose components cover most of the commonly used characters and design a content-reference mapping that fixes the combination of reference set for each character. To establish this mapping function, we firstly decompose each character into a component tree, as shown in Figure 4, based on a commonly used decomposition table<sup>1</sup>. We define the components at the level 0, 1, and 2 as the conspicuous components, which contains both radical and compositional structures that easier be transferred from the references to the target.

**Reference set selection.** This reference set should cover as many conspicuous-level components as possible. Ini-

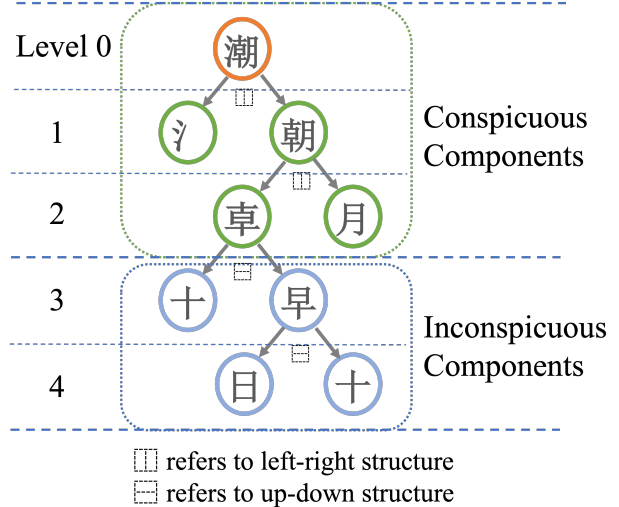


Figure 4. A component tree. To make the mapping process more sensible, the component's structure information is also taken into consideration.

tially, we select a small subset (typically including 100 characters). First, we decompose the characters into component trees. Once the character contains two or more new components, we add this character to our reference set. When the elements in the reference set reach their limits, we stop searching and obtain the style reference set and its corresponding contained components.

**Content-reference mapping.** After completing the reference set selection, we then establish the mapping relations between content glyphs and style references. We propose a greedy process to find  $k$ -shot references for a glyph. In this process, we search the reference set for  $k$  times to establish a mapping relation. During every searching step, we find the reference glyph that shares the most components with the target glyph. If there are multiple solutions, we select the optimal solution that has the most components with the same structure composition. After selection, we remove the reference from the reference set and continue the next searching step. By this process, we can determine every glyph's corresponding  $k$ -shot references.

### 3.5. Training

We train our model to generate the image  $\hat{y}_c$  from a content glyph image  $x_c$  and a fixed set of reference glyph images  $R_s$ . In each iteration, the main branch and the SR branch generate  $\hat{y}_c$  and  $\tilde{y}_c$  simultaneously and are supervised by the same losses. **FSFont** learns the reference encoder  $E_r$ , content encoder  $E_c$ , Style Aggregation Module and decoder  $D$  with following losses: 1) Adversarial loss with the multi-task discriminator. 2) L1 loss among  $\hat{y}_c$ ,  $\tilde{y}_c$  and a paired ground truth image  $y_c$ .

**Adversarial loss.** Since we our aim is to generate visu-

<sup>1</sup><https://github.com/cjkvi/cjkvi-ids/blob/master/ids.txt>

ally high-quality images, we employ a multi-head projection discriminator [22] in our framework. The loss function is represented as follows:

$$\begin{aligned}\mathcal{L}_{adv}^D &= \mathbb{E}_{y_c \in P_d} [\min(0, 1 - D_{s,c}(y_c))] \\ &\quad + \mathbb{E}_{\tilde{y}_c \in P_g} [\min(0, -1 - D_{s,c}(\tilde{y}_c))], \\ \mathcal{L}_{adv}^G &= -\mathbb{E}_{\tilde{y}_c \in P_g} D_{s,c}(\tilde{y}_c),\end{aligned}\quad (7)$$

where  $\tilde{y}_c \in \{\hat{y}_c, \tilde{y}_c\}$ ,  $D_{s,c}(\cdot)$  refers to the logits from the character  $c$  head and style  $s$  head from the discriminator,  $P_g$  denotes the set of generated images from both main branch and Self-Reconstruction branch, and  $P_d$  denotes the set of real glyph images.

**L1 loss.** For learning the pixel-level consistency, we employ an L1 loss between the generated images  $\hat{y}_c$ ,  $\tilde{y}_c$  and ground truth image  $y_c$ .

$$\mathcal{L}_{l1} = \mathbb{E} [\|\hat{y}_c - y_c\|_1 + \|\tilde{y}_c - y_c\|_1]. \quad (8)$$

**Overall objective loss.** Combining all losses mentioned above, we train the whole model by the following objective:

$$\min_G \max_D \lambda_{adv} (\mathcal{L}_{adv}^G + \mathcal{L}_{adv}^D) + \lambda_{l1} \mathcal{L}_{l1}, \quad (9)$$

where  $\lambda_{adv}$  and  $\lambda_{l1}$  are hyperparameters to control the weight of each loss. We empirically set  $\lambda_{adv} = 1$  and  $\lambda_{l1} = 0.1$  in our experiments.

## 4. Experiments

In this section, we evaluate FSFont for the representative Chinese font generation task. We first introduce the datasets we used and compare our framework with other state-of-the-art(SOTA) methods. After that, an ablation study evaluates the effectiveness of each module in our framework and how they affect final results.

### 4.1. Datasets and evaluation metrics

**Datasets.** We choose 407 fonts and 3396 commonly used Chinese characters as our datasets including handwriting fonts, printed fonts as well as artistic fonts. All images are  $128 \times 128$  pixels. We select 100 characters from datasets as our reference set and create a Content-Reference mapping with the strategy discussed in Sec.3.4. Reference set and Content-Reference mapping are fixed in both training set and testing set which means only 100 characters are needed to generate a new font library. The training set contains 397 fonts, 2896 characters. The test set are from 10 representative fonts including typewriter fonts, artistic fonts, and handwriting fonts to evaluate the generalization of our model on variant unseen fonts. We test the methods with two setups *Unseen Fonts Unseen Characters*(UFUC)

and *Unseen Fonts Seen Characters*(UFSC). UFUC refers to the 500 characters in the test fonts, and UFSC refers to the 2896 characters in the test fonts.

**Evaluation metrics.** To evaluate the similarity between generated images and ground truth, we compare our framework with other SOTA methods in the following metrics, i.e. **L1**, **RMSE**, **SSIM** and **LPIPS**. Additionally, we conduct user studies to calculate the **Character Accuracy**, as CNN-based classifiers are tolerant of little defects like missing or broken strokes and blurry edges in a stroke-rich character. We hire 51 volunteers to rigorously count the correct ones from 500 generated characters of each method. A character will be counted as correct only if the volunteer can not spot a defect. For **Style Consistency**, the volunteers are required to evaluate which of the methods generates the most similar character given a set of reference glyph images from 30 randomly selected cases.

### 4.2. Comparison methods

We compare our method with previous SOTA methods. 1) **FUNIT** [18] is a early work on Few-shot image translation in an Unsupervised way which introduces two different encoders and an AdaIN module to generate a new image with mixed content and style. 2) **DG-Font** [31] is an Unsupervised network using Deformable Convolution in Generator to achieve a better effect on cursive characters 3) **MX-Font** [23] adopts multiple experts to extract different local structures which makes cross-lingual generation task possible. 4) **AGIS-net** [8] uses two different decoders to generate images with shape and texture information which makes generated image more stable. 5) **LF-Font** [22] proposes localized style representation which makes it enable to extract the component-wise features. For a fair comparison, we choose the Kaiti Line Font<sup>2</sup> as the standard font and re-train all models on the training datasets in Sec. 4.1.

### 4.3. Experimental results

**Quantitative comparison.** Table 1 shows the FFG performance of our **FSFont** and other competitors. We conducted the experiment on UFUC and UFSC. FSFont clearly outweighs previous SOTA methods on all of the similarity metrics from pixel-level to perceptual-level. On UFSC setup, MX-Font [23] and AGIS-Net [8] generates little more correct characters than FSFont. However, FSFont still generates the most correct characters on UFUC. AGIS-Net suffers from a performance drop on **Character Accuracy** in UFUC. This may suggest that its generalization to new characters are limited. Meanwhile, the user study of **Style Consistency** of FSFont is remarkably better than other methods, which further verifies that FSFont generates the visually similar results from users' perspective.

<sup>2</sup>Font is available at <https://chanind.github.io/hanzi-writer-data/>

Unseen Fonts Seen Characters						
Methods	L1 loss ↓	RMSE ↓	SSIM ↑	LPIPS ↓	User(C) % ↑	User(S) % ↑
FUNIT [18]	0.148	0.344	0.565	0.2543	86.0	0.3
DG-FONT [31]	0.131	0.329	0.604	0.2154	92.4	6.1
MX-FONT [23]	0.152	0.347	0.584	0.2291	<b>97.4</b>	8.4
AGIS-NET [8]	0.105	0.289	0.651	0.1865	97.2	5.2
LF-FONT [22]	0.129	0.322	0.607	0.2006	93.4	11.3
Ours	<b>0.097</b>	<b>0.268</b>	<b>0.671</b>	<b>0.1618</b>	96.6	<b>68.7</b>

Unseen Fonts Unseen Characters						
Methods	L1 loss ↓	RMSE ↓	SSIM ↑	LPIPS ↓	User(C) % ↑	User(S) % ↑
FUNIT [18]	0.152	0.345	0.532	0.2424	84.6	1.2
DG-FONT [31]	0.141	0.341	0.573	0.2151	86.4	3.1
MX-FONT [23]	0.153	0.352	0.573	0.2317	93.2	11.2
AGIS-NET [8]	0.114	0.302	0.623	0.1877	89.8	4.1
LF-FONT [22]	0.138	0.334	0.577	0.2018	90.6	13.3
Ours	<b>0.106</b>	<b>0.283</b>	<b>0.642</b>	<b>0.1627</b>	<b>93.8</b>	<b>67.1</b>

Table 1. Qualitative comparison on UFUC and UFSC datasets

Content	儹	睦	鯤	弦	描	悄	破	谓	舩	纬	徉	豹	妓	揉	锚	访
Reference	<span style="border: 1px solid blue;">儹</span>	<span style="border: 1px solid blue;">睦</span>	<span style="border: 1px solid blue;">鯤</span>	<span style="border: 1px solid blue;">弦</span>	<span style="border: 1px solid blue;">描</span>	<span style="border: 1px solid blue;">悄</span>	<span style="border: 1px solid blue;">破</span>	<span style="border: 1px solid blue;">谓</span>	<span style="border: 1px solid blue;">舩</span>	<span style="border: 1px solid blue;">纬</span>	<span style="border: 1px solid blue;">徉</span>	<span style="border: 1px solid blue;">豹</span>	<span style="border: 1px solid blue;">妓</span>	<span style="border: 1px solid blue;">揉</span>	<span style="border: 1px solid blue;">锚</span>	<span style="border: 1px solid blue;">访</span>
FUNIT	儹	睦	鯤	弦	描	悄	破	谓	舩	纬	徉	豹	妓	揉	锚	访
MX-Font	儹	睦	鯤	弦	描	悄	破	谓	舩	纬	徉	豹	妓	揉	锚	访
DG-Font	儹	睦	鯤	弦	描	悄	破	谓	舩	纬	徉	豹	妓	揉	锚	访
AGIS-Net	儹	睦	鯤	弦	描	悄	破	谓	舩	纬	徉	豹	妓	揉	锚	访
LF-Font	儹	睦	鯤	弦	描	悄	破	谓	舩	纬	徉	豹	妓	揉	锚	访
Ours	儹	睦	鯤	弦	描	悄	破	谓	舩	纬	徉	豹	妓	揉	锚	访
GT	儹	睦	鯤	弦	描	悄	破	谓	舩	纬	徉	豹	妓	揉	锚	访

Figure 5. Generated results of each method on UFUC datasets. We represent the generated samples of four different kinds of fonts. We mark the main component of each character with boxes. The blue boxes in Reference are components we hope the model recover. It shows our model (green boxes) is capable of recovering more details from Reference than other SOTA works do (red boxes).

**Qualitative comparison** We illustrate the generated samples in Figure 5 for each method. We selected four different fonts including typewriter fonts, artistic fonts as well as handwriting fonts to see the generalization of all competitors. As demonstrated in Figure 5, FSFont are available to recover as many details from reference images. Though other methods like LF-Font [22] or AGIS-Net [8] are able to generate stable characters and recover coarse features such as the thickness of strokes and inclination of font, they could not recover details as explicitly as our method does.

**Ablation studies.** In this part, we discuss the effectiveness of each module we introduce in FSFont. We discard

each module at a time and train the model with other settings unchanged. The overall evaluation results on UFUC datasets are shown in Table 2. We replace SAM with averaging features in  $F_r$  to test its effect. For Reference Selection and Content-Reference mapping, we replace them with the strategy of LF-Font [22] by randomly selecting reference glyph images with a common component set for each content character. Both two modules have a positive effect on the final results. The Self-Reconstruction Branch has a significant impact on outputs. As shown in Table 3, the model trained without SR branch can hardly recover details from reference glyph images.

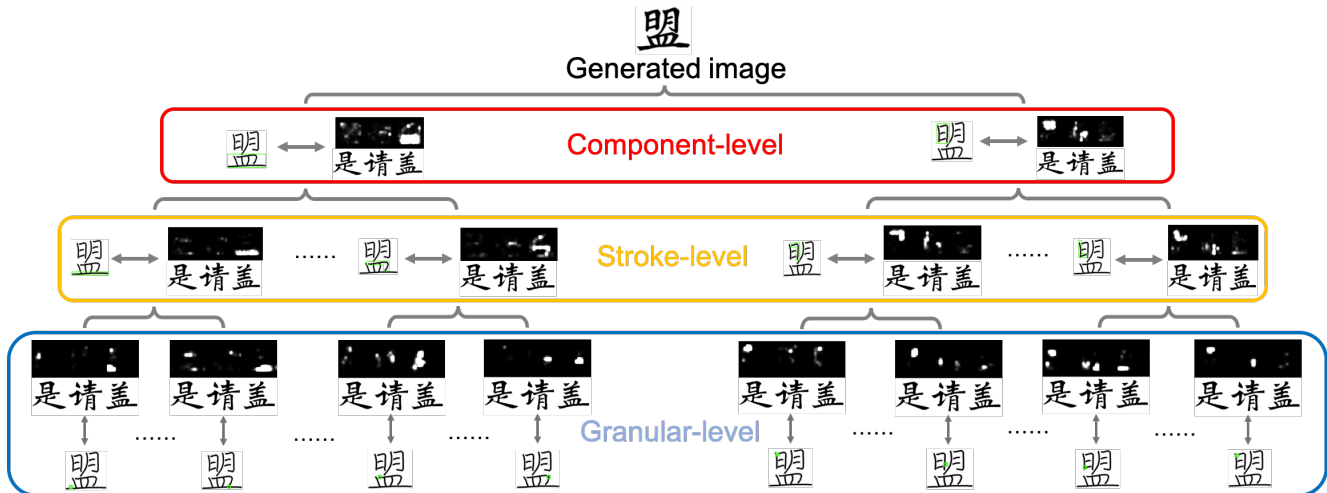


Figure 6. **Visualization of Style Aggregation Module.** The brighter spot in the attention maps denotes the larger contribution of corresponding features in the reference feature maps. The light-green dot, line and bounding box denote the queries from different level.

Unseen Fonts Unseen Characters						
SAM	SR	RS	L1 loss ↓	RMSE ↓	SSIM ↑	LPIPS ↓
✓	✓	✓	<b>0.106</b>	<b>0.283</b>	<b>0.642</b>	<b>0.1627</b>
✗	✓	✓	0.113	0.294	0.621	0.1822
✓	✗	✓	0.127	0.318	0.596	0.1859
✓	✓	✗	0.114	0.292	0.624	0.1798
✗	✗	✗	0.131	0.338	0.584	0.2189

Table 2. **Analysis of different modules in our proposed framework.** By discarding the Style Aggregation Module (SAM), Self Construction (SR), and Reference Selection (RS) individually, we can see that all these modules have positive effects on the original model respectively. The model with three modules has the best performance in all evaluation metrics.

Content	排	怯	波	鲤	娃	遮
Reference	把	快	没	蛟	好	还
w/o SR	排	怯	波	鲤	娃	遮
with SR	排	怯	波	鲤	娃	遮
GT	排	怯	波	鲤	娃	遮

Table 3. **Comparison of generated images with and without Self-Reconstruction branch.** The green box in the reference set is the component we hope the model to recover. The red box shows the insufficient details generated from the model trained without Self Reconstruction branch.

**Visualization of SAM.** To demonstrate the effectiveness of SAM, we visualize the attention maps for different levels in Figure 6. Specifically, given a certain spatial point  $q$  in the content feature map as a query, we can obtain the corresponding correlations  $A_q^m \in \mathbb{R}^{khw}$  from the spatial correspondence matrix  $A^m \in \mathbb{R}^{hw \times khw}$ , and construct an attention map by reshaping  $A_q^m$  to  $h \times kw$ . We consider the queries from the **Granular**, **Stroke**, and **Component-level**, respectively, and compute the final attention map by summing over the attention maps related to the queries. It shows that our SAM module empowers the model to attend to the correct *FLS*s from reference images and extract a sub-component level feature representation for content images.

## 5. Conclusion

In this paper, we propose a novel FFG model, which is able to calculate the spatial correspondence of the content and reference based on their component features. Our proposed Style Aggregation Module aggregates fine-grained local styles of references to content’s corresponding location with high-fidelity. Besides, we propose a Self-Reconstruction branch to help model to recover details from references. Last but not least, our Reference Selection strategy guarantee that each content can match references that share common conspicuous components. Our extensive experiments show that FSFont significantly outperforms other methods in both objective and subjective similarity. **Limitation** The model is trained on limited data, it can not faithfully replicate every detail of the font. **Negative Impact** Though FSFont can be potentially used to imitate handwriting, a human expert can still spot the difference between generated and real handwritings.



## References

- [1] Samaneh Azadi, Matthew Fisher, Vladimir G Kim, Zhaowen Wang, Eli Shechtman, and Trevor Darrell. Multi-content gan for few-shot font style transfer. In *Proceedings of the IEEE conference on computer vision and pattern recognition*, pages 7564–7573, 2018. 3
- [2] Kyungjune Baek, Yunjey Choi, Youngjung Uh, Jaejun Yoo, and Hyunjung Shim. Rethinking the truly unsupervised image-to-image translation. In *Proceedings of the IEEE/CVF International Conference on Computer Vision (ICCV)*, pages 14154–14163, October 2021. 3
- [3] Ankan Kumar Bhunia, Salman Khan, Hisham Cholakkal, Rao Muhammad Anwer, Fahad Shahbaz Khan, and Mubarak Shah. Handwriting transformers. *arXiv preprint arXiv:2104.03964*, 2021. 3
- [4] Junbum Cha, Sanghyuk Chun, Gayoung Lee, Bado Lee, Seonghyeon Kim, and Hwalsuk Lee. Few-shot compositional font generation with dual memory. In *Computer Vision–ECCV 2020: 16th European Conference, Glasgow, UK, August 23–28, 2020, Proceedings, Part XIX 16*, pages 735–751. Springer, 2020. 1, 2, 3
- [5] Jie Chang, Yujun Gu, Ya Zhang, Yan-Feng Wang, and CM Innovation. Chinese handwriting imitation with hierarchical generative adversarial network. In *BMVC*, page 290, 2018. 2, 13
- [6] Yunjey Choi, Minje Choi, Munyoung Kim, Jung-Woo Ha, Sungjun Kim, and Jaegul Choo. Stargan: Unified generative adversarial networks for multi-domain image-to-image translation. In *Proceedings of the IEEE conference on computer vision and pattern recognition*, pages 8789–8797, 2018. 2
- [7] Yunjey Choi, Youngjung Uh, Jaejun Yoo, and Jung-Woo Ha. Stargan v2: Diverse image synthesis for multiple domains. In *Proceedings of the IEEE/CVF Conference on Computer Vision and Pattern Recognition*, pages 8188–8197, 2020. 2
- [8] Yue Gao, Yuan Guo, Zhouhui Lian, Yingmin Tang, and Jianguo Xiao. Artistic glyph image synthesis via one-stage few-shot learning. *ACM Transactions on Graphics (TOG)*, 38(6):1–12, 2019. 1, 2, 3, 6, 7
- [9] Yiming Gao and Jiangqin Wu. Gan-based unpaired chinese character image translation via skeleton transformation and stroke rendering. In *Proceedings of the AAAI Conference on Artificial Intelligence*, volume 34, pages 646–653, 2020. 2, 3
- [10] Ian Goodfellow, Jean Pouget-Abadie, Mehdi Mirza, Bing Xu, David Warde-Farley, Sherjil Ozair, Aaron Courville, and Yoshua Bengio. Generative adversarial nets. *Advances in neural information processing systems*, 27, 2014. 1
- [11] Ammar Ul Hassan, Hammad Ahmed, and Jaeyoung Choi. Unpaired font family synthesis using conditional generative adversarial networks. *Knowledge-Based Systems*, 229:107304, 2021. 2, 3
- [12] Xun Huang and Serge Belongie. Arbitrary style transfer in real-time with adaptive instance normalization. In *Proceedings of the IEEE International Conference on Computer Vision*, pages 1501–1510, 2017. 2
- [13] Yaoxiong Huang, Mengchao He, Lianwen Jin, and Yongpan Wang. Rd-gan: few/zero-shot chinese character style transfer via radical decomposition and rendering. In *European Conference on Computer Vision*, pages 156–172. Springer, 2020. 2, 3
- [14] Phillip Isola, Jun-Yan Zhu, Tinghui Zhou, and Alexei A Efros. Image-to-image translation with conditional adversarial networks. In *Proceedings of the IEEE conference on computer vision and pattern recognition*, pages 1125–1134, 2017. 1, 2
- [15] Yue Jiang, Zhouhui Lian, Yingmin Tang, and Jianguo Xiao. Dcfont: an end-to-end deep chinese font generation system. In *SIGGRAPH Asia 2017 Technical Briefs*, pages 1–4. 2017. 2
- [16] Yue Jiang, Zhouhui Lian, Yingmin Tang, and Jianguo Xiao. Scfont: Structure-guided chinese font generation via deep stacked networks. In *Proceedings of the AAAI conference on artificial intelligence*, volume 33, pages 4015–4022, 2019. 2, 3
- [17] Alexander H Liu, Yen-Cheng Liu, Yu-Ying Yeh, and Yu-Chiang Frank Wang. A unified feature disentangler for multi-domain image translation and manipulation. *arXiv preprint arXiv:1809.01361*, 2018. 2
- [18] Ming-Yu Liu, Xun Huang, Arun Mallya, Tero Karras, Timo Aila, Jaakko Lehtinen, and Jan Kautz. Few-shot unsupervised image-to-image translation. In *Proceedings of the IEEE/CVF International Conference on Computer Vision*, pages 10551–10560, 2019. 2, 6, 7, 13
- [19] Pengyuan Lyu, Xiang Bai, Cong Yao, Zhen Zhu, Tengpeng Huang, and Wenyu Liu. Auto-encoder guided gan for chinese calligraphy synthesis. In *2017 14th IAPR International Conference on Document Analysis and Recognition (ICDAR)*, volume 1, pages 1095–1100. IEEE, 2017. 2
- [20] Mehdi Mirza and Simon Osindero. Conditional generative adversarial nets. *arXiv preprint arXiv:1411.1784*, 2014. 1
- [21] Takeru Miyato and Masanori Koyama. cgans with projection discriminator, 2018. 4
- [22] Song Park, Sanghyuk Chun, Junbum Cha, Bado Lee, and Hyunjung Shim. Few-shot font generation with localized style representations and factorization. *arXiv preprint arxiv:2009.11042*, 2020. 1, 2, 3, 5, 6, 7, 13
- [23] Song Park, Sanghyuk Chun, Junbum Cha, Bado Lee, and Hyunjung Shim. Multiple heads are better than one: Few-shot font generation with multiple localized experts. *arXiv preprint arXiv:2104.00887*, 2021. 1, 2, 3, 6, 7, 13
- [24] Donghui Sun, Qing Zhang, and Jun Yang. Pyramid embedded generative adversarial network for automated font generation. In *2018 24th International Conference on Pattern Recognition (ICPR)*, pages 976–981. IEEE, 2018. 2
- [25] Yuchen Tian. Rewrite: Neural style transfer for chinese fonts. <https://github.com/kaonashi-tyc/Rewrite>, 2016. 2
- [26] Yuchen Tian. zi2zi: Master chinese calligraphy with conditional adversarial networks. <https://github.com/kaonashi-tyc/zi2zi>, 2017. 1, 2
- [27] Ashish Vaswani, Noam Shazeer, Niki Parmar, Jakob Uszkoreit, Llion Jones, Aidan N Gomez, Łukasz Kaiser, and Illia Polosukhin. Attention is all you need. In *Advances in neural*

*information processing systems*, pages 5998–6008, 2017. [3](#), [4](#)

- [28] Chuan Wen, Yujie Pan, Jie Chang, Ya Zhang, Siheng Chen, Yanfeng Wang, Mei Han, and Qi Tian. Handwritten chinese font generation with collaborative stroke refinement. In *Proceedings of the IEEE/CVF Winter Conference on Applications of Computer Vision*, pages 3882–3891, 2021. [2](#)
- [29] Qi Wen, Shuang Li, Bingfeng Han, and Yi Yuan. Zigan: Fine-grained chinese calligraphy font generation via a few-shot style transfer approach. *arXiv preprint arXiv:2108.03596*, 2021. [3](#)
- [30] Shan-Jean Wu, Chih-Yuan Yang, and Jane Yung-jen Hsu. Calligan: Style and structure-aware chinese calligraphy character generator. *arXiv preprint arXiv:2005.12500*, 2020. [2](#)
- [31] Yangchen Xie, Xinyuan Chen, Li Sun, and Yue Lu. Dg-font: Deformable generative networks for unsupervised font generation. In *Proceedings of the IEEE/CVF Conference on Computer Vision and Pattern Recognition*, pages 5130–5140, 2021. [1](#), [2](#), [3](#), [6](#), [7](#), [13](#)
- [32] Xiaoming Yu, Yuanqi Chen, Thomas Li, Shan Liu, and Ge Li. Multi-mapping image-to-image translation via learning disentanglement. *arXiv preprint arXiv:1909.07877*, 2019. [2](#)
- [33] Yexun Zhang, Ya Zhang, and Wenbin Cai. Separating style and content for generalized style transfer. In *Proceedings of the IEEE conference on computer vision and pattern recognition*, pages 8447–8455, 2018. [3](#)
- [34] Jun-Yan Zhu, Taesung Park, Phillip Isola, and Alexei A Efros. Unpaired image-to-image translation using cycle-consistent adversarial networks. In *Proceedings of the IEEE international conference on computer vision*, pages 2223–2232, 2017. [2](#)

## References

- [1] Samaneh Azadi, Matthew Fisher, Vladimir G Kim, Zhaowen Wang, Eli Shechtman, and Trevor Darrell. Multi-content gan for few-shot font style transfer. In *Proceedings of the IEEE conference on computer vision and pattern recognition*, pages 7564–7573, 2018. [3](#)
- [2] Kyungiune Baek, Yunjey Choi, Youngjung Uh, Jaejun Yoo, and Hyunjung Shim. Rethinking the truly unsupervised image-to-image translation. In *Proceedings of the IEEE/CVF International Conference on Computer Vision (ICCV)*, pages 14154–14163, October 2021. [3](#)
- [3] Ankan Kumar Bhunia, Salman Khan, Hisham Cholakkal, Rao Muhammad Anwer, Fahad Shahbaz Khan, and Mubarak Shah. Handwriting transformers. *arXiv preprint arXiv:2104.03964*, 2021. [3](#)
- [4] Junbum Cha, Sanghyuk Chun, Gayoung Lee, Bado Lee, Seonghyeon Kim, and Hwalsuk Lee. Few-shot compositional font generation with dual memory. In *Computer Vision–ECCV 2020: 16th European Conference, Glasgow, UK, August 23–28, 2020, Proceedings, Part XIX 16*, pages 735–751. Springer, 2020. [1](#), [2](#), [3](#)
- [5] Jie Chang, Yujun Gu, Ya Zhang, Yan-Feng Wang, and CM Innovation. Chinese handwriting imitation with hierarchical generative adversarial network. In *BMVC*, page 290, 2018. [2](#), [13](#)

- [6] Yunjey Choi, Minje Choi, Munyoung Kim, Jung-Woo Ha, Sunghun Kim, and Jaegul Choo. Stargan: Unified generative adversarial networks for multi-domain image-to-image translation. In *Proceedings of the IEEE conference on computer vision and pattern recognition*, pages 8789–8797, 2018. [2](#)
- [7] Yunjey Choi, Youngjung Uh, Jaejun Yoo, and Jung-Woo Ha. Stargan v2: Diverse image synthesis for multiple domains. In *Proceedings of the IEEE/CVF Conference on Computer Vision and Pattern Recognition*, pages 8188–8197, 2020. [2](#)
- [8] Yue Gao, Yuan Guo, Zhouhui Lian, Yingmin Tang, and Jianguo Xiao. Artistic glyph image synthesis via one-stage few-shot learning. *ACM Transactions on Graphics (TOG)*, 38(6):1–12, 2019. [1](#), [2](#), [3](#), [6](#), [7](#)
- [9] Yiming Gao and Jiangqin Wu. Gan-based unpaired chinese character image translation via skeleton transformation and stroke rendering. In *Proceedings of the AAAI Conference on Artificial Intelligence*, volume 34, pages 646–653, 2020. [2](#), [3](#)
- [10] Ian Goodfellow, Jean Pouget-Abadie, Mehdi Mirza, Bing Xu, David Warde-Farley, Sherjil Ozair, Aaron Courville, and Yoshua Bengio. Generative adversarial nets. *Advances in neural information processing systems*, 27, 2014. [1](#)
- [11] Ammar Ul Hassan, Hammad Ahmed, and Jaeyoung Choi. Unpaired font family synthesis using conditional generative adversarial networks. *Knowledge-Based Systems*, 229:107304, 2021. [2](#), [3](#)
- [12] Xun Huang and Serge Belongie. Arbitrary style transfer in real-time with adaptive instance normalization. In *Proceedings of the IEEE International Conference on Computer Vision*, pages 1501–1510, 2017. [2](#)
- [13] Yaoxiong Huang, Mengchao He, Lianwen Jin, and Yongpan Wang. Rd-gan: few/zero-shot chinese character style transfer via radical decomposition and rendering. In *European Conference on Computer Vision*, pages 156–172. Springer, 2020. [2](#), [3](#)
- [14] Phillip Isola, Jun-Yan Zhu, Tinghui Zhou, and Alexei A Efros. Image-to-image translation with conditional adversarial networks. In *Proceedings of the IEEE conference on computer vision and pattern recognition*, pages 1125–1134, 2017. [1](#), [2](#)
- [15] Yue Jiang, Zhouhui Lian, Yingmin Tang, and Jianguo Xiao. Dcfont: an end-to-end deep chinese font generation system. In *SIGGRAPH Asia 2017 Technical Briefs*, pages 1–4, 2017. [2](#)
- [16] Yue Jiang, Zhouhui Lian, Yingmin Tang, and Jianguo Xiao. Sefont: Structure-guided chinese font generation via deep stacked networks. In *Proceedings of the AAAI conference on artificial intelligence*, volume 33, pages 4015–4022, 2019. [2](#), [3](#)
- [17] Alexander H Liu, Yen-Cheng Liu, Yu-Ying Yeh, and Yu-Chiang Frank Wang. A unified feature disentangler for multi-domain image translation and manipulation. *arXiv preprint arXiv:1809.01361*, 2018. [2](#)
- [18] Ming-Yu Liu, Xun Huang, Arun Mallya, Tero Karras, Timo Aila, Jaakko Lehtinen, and Jan Kautz. Few-shot unsupervised image-to-image translation. In *Proceedings of the*

- IEEE/CVF International Conference on Computer Vision*, pages 10551–10560, 2019. 2, 6, 7, 13
- [19] Pengyuan Lyu, Xiang Bai, Cong Yao, Zhen Zhu, Tengpeng Huang, and Wenyu Liu. Auto-encoder guided gan for chinese calligraphy synthesis. In *2017 14th IAPR International Conference on Document Analysis and Recognition (ICDAR)*, volume 1, pages 1095–1100. IEEE, 2017. 2
- [20] Mehdi Mirza and Simon Osindero. Conditional generative adversarial nets. *arXiv preprint arXiv:1411.1784*, 2014. 1
- [21] Takeru Miyato and Masanori Koyama. cgans with projection discriminator, 2018. 4
- [22] Song Park, Sanghyuk Chun, Junbum Cha, Bado Lee, and Hyunjung Shim. Few-shot font generation with localized style representations and factorization. *arXiv preprint arxiv:2009.11042*, 2020. 1, 2, 3, 5, 6, 7, 13
- [23] Song Park, Sanghyuk Chun, Junbum Cha, Bado Lee, and Hyunjung Shim. Multiple heads are better than one: Few-shot font generation with multiple localized experts. *arXiv preprint arXiv:2104.00887*, 2021. 1, 2, 3, 6, 7, 13
- [24] Donghui Sun, Qing Zhang, and Jun Yang. Pyramid embedded generative adversarial network for automated font generation. In *2018 24th International Conference on Pattern Recognition (ICPR)*, pages 976–981. IEEE, 2018. 2
- [25] Yuchen Tian. Rewrite: Neural style transfer for chinese fonts. <https://github.com/kaonashi-tyc/Rewrite>, 2016. 2
- [26] Yuchen Tian. zi2zi: Master chinese calligraphy with conditional adversarial networks. <https://github.com/kaonashi-tyc/zi2zi>, 2017. 1, 2
- [27] Ashish Vaswani, Noam Shazeer, Niki Parmar, Jakob Uszkoreit, Llion Jones, Aidan N Gomez, Łukasz Kaiser, and Illia Polosukhin. Attention is all you need. In *Advances in neural information processing systems*, pages 5998–6008, 2017. 3, 4
- [28] Chuan Wen, Yujie Pan, Jie Chang, Ya Zhang, Siheng Chen, Yanfeng Wang, Mei Han, and Qi Tian. Handwritten chinese font generation with collaborative stroke refinement. In *Proceedings of the IEEE/CVF Winter Conference on Applications of Computer Vision*, pages 3882–3891, 2021. 2
- [29] Qi Wen, Shuang Li, Bingfeng Han, and Yi Yuan. Zigan: Fine-grained chinese calligraphy font generation via a few-shot style transfer approach. *arXiv preprint arXiv:2108.03596*, 2021. 3
- [30] Shan-Jean Wu, Chih-Yuan Yang, and Jane Yung-jen Hsu. Calligan: Style and structure-aware chinese calligraphy character generator. *arXiv preprint arXiv:2005.12500*, 2020. 2
- [31] Yangchen Xie, Xinyuan Chen, Li Sun, and Yue Lu. Dg-font: Deformable generative networks for unsupervised font generation. In *Proceedings of the IEEE/CVF Conference on Computer Vision and Pattern Recognition*, pages 5130–5140, 2021. 1, 2, 3, 6, 7, 13
- [32] Xiaoming Yu, Yuanqi Chen, Thomas Li, Shan Liu, and Ge Li. Multi-mapping image-to-image translation via learning disentanglement. *arXiv preprint arXiv:1909.07877*, 2019. 2
- [33] Yexun Zhang, Ya Zhang, and Wenbin Cai. Separating style and content for generalized style transfer. In *Proceedings of the IEEE conference on computer vision and pattern recognition*, pages 8447–8455, 2018. 3
- [34] Jun-Yan Zhu, Taesung Park, Phillip Isola, and Alexei A Efros. Unpaired image-to-image translation using cycle-consistent adversarial networks. In *Proceedings of the IEEE international conference on computer vision*, pages 2223–2232, 2017. 2

## Appendices

### A. Implementation Details

#### A.1. Reference Selection

In this section, we will discuss the implementation details of reference selection, which can be divided into two steps: **reference set determination** and **content-reference mapping**.

**Reference set determination** As mentioned in paper’s section 3.4, our target is to search for a reference glyph set which covers the most conspicuous-level components, and our detailed algorithm can be demonstrated by Algorithm 1. In our algorithm,  $X$  denotes the entire character list sorted by glyphs’ occurrence frequency, whose total capacity is 20K.  $T$  denotes the single level decomposition look-up tables for all characters in  $X$ . For one key  $x_i$  in  $T$ , their corresponding value  $\chi_i$  is a subset of  $X$ , consisting of their decomposing components’ name list and corresponding decomposing form. By exploring this components list, we employ breadth first search to recursively obtain all the components at different levels, which forming the component tree in our work.  $C$  denotes the set that contains all conspicuous-level components, whose total capacity is 374.  $N_{ref}$  denotes the total capacity of our target reference set, which is fixed to 100 in our experiments.

As an initialization, we set our target reference set  $\hat{U}$  and corresponding covering components  $\hat{C}$  as  $\emptyset$ . Then we begin searching process in  $X$ . For every glyph  $x_i$  in  $X$ , we obtain its conspicuous-level components  $c_i$  via the function *searchComponents* in 1. If there is unique components in  $c_i$  which is not in current component pool  $\hat{C}$ , we regard this glyph  $x_i$  as our target reference glyph, and we add it and its unique components to  $\hat{U}$  and  $\hat{C}$  respectively. In our experiment, we ensure that every latest adding reference have 2 or more unique components. Once the capacity of  $\hat{U}$  reaches  $N_{ref}$ , we terminate the searching process.

**Content-reference mapping** Since we have determined the reference set. It’s more convenient for us to find the mapping relationship between a arbitrary glyph and its references whose conspicuous components are in common. For  $k$ -shot reference mapping (one content glyph corresponds to  $k$  style references), we do the following searching process for  $k$  times: We find the glyph in reference set which share the most conspicuous component, and remove it from the original reference set. If there is multiple choice, we leave the one whose component’s composition form is the same with the content glyph.

We show some of the finding mappings between content and references in Fig. 8.

---

#### Algorithm 1: Reference set selection

---

**input** :  $X = \{x_i\}$ : Common-used glyph list.  
 $T = \{x_i : \chi_i\}$ : Single-level decomposition look-up table.  $\chi_i \subset X$ .  
 $C$ : Conspicuous-level component set.  
 $N_{ref}$ : Max capacity of Reference set.  
 $d$ : Max search depth in component tree.  
**output**:  $\hat{U}$ : Reference set.  
 $\hat{C}$ : All components which  $U$  can cover.

**Function** *searchComponents* ( $x_i$ ) :

```
queue  $\leftarrow$   $\{x_i\}$ ;  $i \leftarrow 0$ ;  $c_i \leftarrow \emptyset$ 
repeat
  queue*  $\leftarrow$   $\emptyset$ 
  for  $x \in$  queue do
    queue*  $\leftarrow$  queue*  $\cup$   $T(x)$ 
     $c_i \leftarrow T(x) \cap C$ 
  end
  queue  $\leftarrow$  queue*;  $i \leftarrow i + 1$ 
until  $i \geq d$ ;
return  $c_i$ 
```

**End Function**

**Function** *Main* () :

```
 $\hat{U} \leftarrow \emptyset$ ;  $\hat{C} \leftarrow \emptyset$ 
for  $x_i \in X$  do
   $c_i \leftarrow$  searchComponents( $x_i$ )
  if  $\exists \hat{c} \in c_i$  s.t.  $\hat{c} \notin \hat{C}$  then  $\hat{C} \leftarrow \hat{C} \cup c_i$ ,
  add  $x_i$  to  $\hat{U}$ ;
  if  $Len(\hat{U}) \geq N_{ref}$  then break;
end
return  $\hat{U}$ ,  $\hat{C}$ 
```

**End Function**

---

#### A.2. Model Architecture

Our entire model can be divided into two parts: the generator and discriminator. Both of them are built up of two typical types of blocks: the Convolution block and the Residual block, which are illustrated in Fig 7. The Residual block contains two identical Convolution blocks. Since the Residual block has its own downsampling operator, its Convolution blocks skip the downsampling step.

**Generator** As mentioned in our method, the generator model consists of three respective modules: reference encoder  $E_r$ , content encoder  $E_c$ , and decoder  $D$ . Both  $E_r$  and  $E_c$  are also made up of the following two types of blocks: the Convolution block and Residual block. The detailed architecture is illustrated in Table. 4.

**Discriminator** The discriminator is also made up of the Convolution block and the Residual block. In Discriminator, each Convolution and Residual block is followed by a

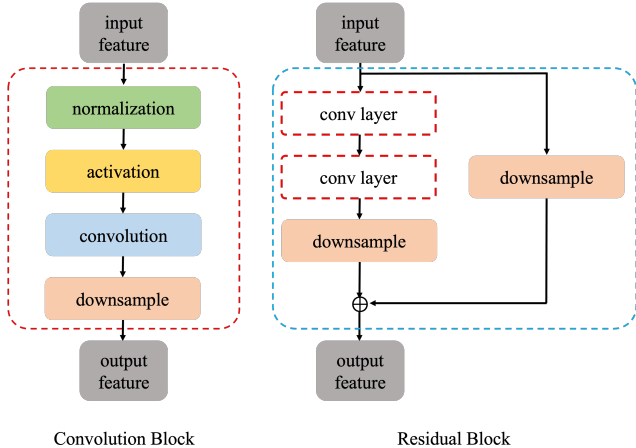


Figure 7. Structures of the Convolution Block and the Residual Block in Tab.4

spectral normalization. The detailed architecture is illustrated in Table. 4.

### A.3. Training details

We use Adam optimizer to optimize the FSFont’s parameters. The generator and discriminator’s learning rates are 0.0002 and 0.0008, respectively. Kaiming initialization is applied for the model. During training, by default we set the reference to be 3-shot for training. If one glyph’s reference set’s capacity is less than 3, we duplicate one of reference glyph until the capacity equals to 3 for purpose of batch training. In our proposed SAM, empirically we set number of attention heads to be 8 and batch size to be 32. We train our model with full objective function for 500k iterations.

## B. Additional Experimental Results

In Fig.8, we demonstrate more experimental results on unseen fonts. The results show that FSFont can deal with variant font styles, including typewriter fonts, artistic fonts, and handwriting fonts. In addition, we show the content font we used in our experiment in Fig.9.

We also demonstrate more visualization results about the attention maps in Fig. 10. We show the attention maps on characters with variant structures. It is shown that the attention is able to capture the correct correspondence in different structures.

## C. User Study Examples

We show the sample images used for the user study in Fig.11 and Fig.12. A content image, a reference set, and shuffled results from five methods, i.e. FUNIT [18], AG-ISNet [5], LF-Font [22], DFFont [31], MX-Font [23], and FSFont, are displayed to users for every query. Users are

required to choose the most consistent one according the style of the reference set. As the orders of the methods are shuffled, we also provide the answers for each case.

<b>Reference Encoder <math>E_r</math></b>							
Layer Type	Normalization	Activation	Padding	Kernel Size	Stride	Downsample	Feature maps
Convolution block	IN	ReLU	1	3	1	-	32
Convolution block	IN	ReLU	1	3	1	AvgPool	64
Convolution block	IN	ReLU	1	3	1	AvgPool	128
Residual block	IN	ReLU	1	3	1	-	128
Residual block	IN	ReLU	1	3	1	-	128
Residual block	IN	ReLU	1	3	1	AvgPool	256
Residual block	IN	ReLU	1	3	1	-	256
Output Layer	-	Sigmoid	-	-	-	-	256

<b>Content Encoder <math>E_c</math></b>							
Layer Type	Normalization	Activation	Padding	Kernel Size	Stride	Downsample	Feature maps
Convolution block	IN	ReLU	1	3	1	-	32
Convolution block	IN	ReLU	1	3	2	-	64
Convolution block	IN	ReLU	1	3	2	-	128
Convolution block	IN	ReLU	1	3	2	-	256
Convolution block	IN	ReLU	1	3	1	-	256

<b>Decoder <math>D</math></b>							
Layer Type	Normalization	Activation	Padding	Kernel Size	Stride	Upsample	Feature maps
Residual block	IN	ReLU	1	3	1	-	256
Residual block	IN	ReLU	1	3	1	-	256
Residual block	IN	ReLU	1	3	1	-	256
Convolution block	IN	ReLU	1	3	1	Nearest	128
Convolution block	IN	ReLU	1	3	1	Nearest	64
Convolution block	IN	ReLU	1	3	1	Nearest	32
Convolution block	IN	ReLU	1	3	1	-	1
Output Layer	-	Sigmoid	-	-	-	-	1

<b>Discriminator <math>D</math></b>							
Layer Type	Normalization	Activation	Padding	Kernel Size	Stride	Downsample	Feature maps
Convolution block	IN	-	1	3	2	-	32
Residual block	IN	ReLU	1	3	1	AvgPool	64
Residual block	IN	ReLU	1	3	1	AvgPool	128
Residual block	IN	ReLU	1	3	1	AvgPool	256
Residual block	IN	ReLU	1	3	1	-	256
Residual block	IN	ReLU	1	3	1	AdaAvgPool	512
Output layer	Multi-task embedding						

Table 4. **Architecture of the generator modules  $E_r$ ,  $E_c$ ,  $D$  and the discriminator.** Convolution block and Residual block denote the module mentioned in Fig 7. IN denotes instance normalization. All padding operation is zero-padding. AvgPool and AdaptiveAvgPool denotes average pooling and adaptive average pooling. In discriminator’s output layer, we use two embedding operators to embed the output feature map into two prediction vector of the font style and the character’s name.

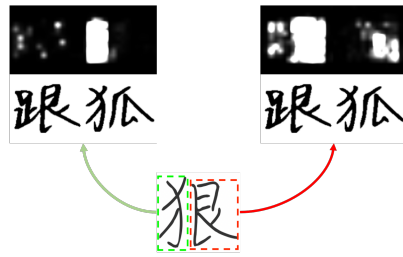
Content	Reference	Generate	GT	Content	Reference	Generate	GT
剧	呢别卖	剧	剧	剧	呢别卖	剧	剧
咪	说和	咪	咪	忘	就想甩	忘	忘
连	转还	连	连	徂	组得	徂	徂
约	组的	约	约	意	是想亲	意	意
焦	焦你	焦	焦	弦	就张累	弦	弦
媪	好去累	媪	媪	描	把累菜	描	描
底	的度舐	底	底	绀	组疝	绀	绀
完	下家祝	完	完	轻	没转差	轻	轻
估	你喻装	估	估	叠	没带组	叠	叠
昙	是去那	昙	昙	褪	还跟被	褪	褪
备	峰累	备	备	歌	啊次灯	歌	歌
悻	累快请	悻	悻	静	请你建	静	静
餌	鲫饭	餌	餌	药	的菜组	药	药
谓	请累	谓	谓	逛	还弄狐	逛	逛
洳	啊好没	洳	洳	魏	和好魁	魏	魏
锱	啊亲钟	锱	锱	炸	酢灯	炸	炸
猓	岁罪狐	猓	猓	砍	次码	砍	砍
超	起啊那	超	超	保	你和	保	保
房	咋下放	房	房	杰	和焦	杰	杰
鞋	去鞞	鞋	鞋	狗	的啊狐	狗	狗

Figure 8. More Results. This Figure shows the Content-Reference mapping and generated results on all test fonts.

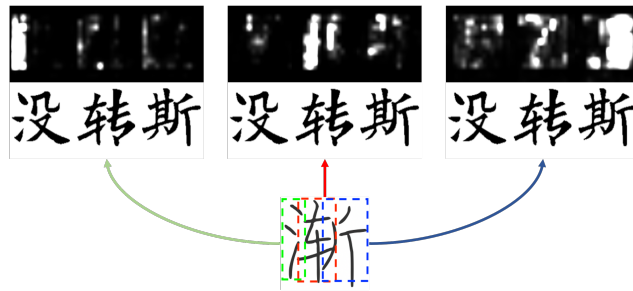
图抢娅钛伫鳞赝萦阎么骠纭仓计缙缝傲动迟脍  
 垒项诤掩鹄焕鹄灏屈乐飙匱垝铍均邝噤层镌驪  
 鸚变矧尘躐项饺罚谤丝荡敌鹅僚莠摺颇晓鲟谀  
 脓郟矸恢窍滦册嵘貳见鵠议铈掳缙缙维钦跣榉  
 驷圻噉鸱辽胼枉轳盐苜苒诔苇鸢啮蛲滚汧鳖镍铸  
 绉熇头狎浑带喜匀黠洼嫫毳钹农掷涛鲑臬拣淮轩饼瞩  
 桥腾减陕钩奋戆轳设忆纒紧农掷涛鲑臬拣淮轩饼瞩  
 緄骤鸯纒专论吓葜务佻鹏鲨呕冥赏癃签潇呛赢砗  
 贮铐缙竞趋楮臙态碇暮馗鹑飘临谜蔚荆渗媛产饩  
 问纹咻炅呜巅将盗帜钼隍簧椽酝预鰈浅菘鏢导馁  
 卜猫执贯脏驻寝汤拔鹜钙蹕搥渍祸阔坠许涡戈  
 犹员酱掣恼惭启萆样说麸抡溲躡戩详蚩癞尧录  
 吟轔诚鲛恼惭启萆样说麸抡溲躡戩详蚩癞尧录  
 贿帅剪鰳碎滤叹兽猕鳧嚶断诩玃缓讶脍赖锰捞

Figure 9. The content font we used in our experiment.

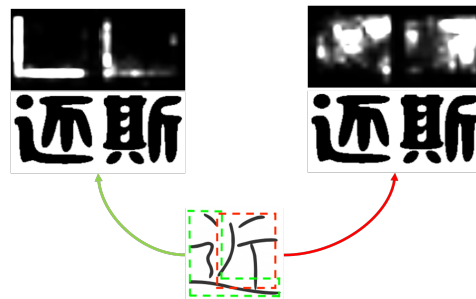




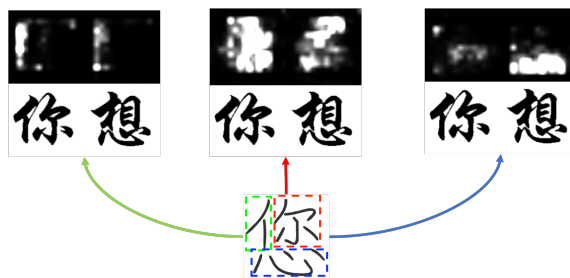
(a) Left-Right structure



(b) Left-Middle-Right structure



(c) Half-Surrounded Structure



(d) Compound Structure (Left-Right + Top-down)

Figure 10. **Visualization on Attention maps.** This Figure shows the attention maps given the different regions in content glyph.

content	强	纸	床	怎	催	崔	吹	客	坑	话	冯	连	法	拍	伟
reference	啊	舐	和	想	你	岁	喻	啊	就	和	次	远	没	的	你
	张	组	度	醉	岁	焦	冷	家	凯	说	吗	转	去	是	韩
	蛮				焦			峰	去	卖				把	
A	强	纸	床	怎	催	崔	吹	客	坑	话	冯	连	法	拍	伟
B	强	纸	床	怎	催	崔	吹	客	坑	话	冯	连	法	拍	伟
C	强	纸	床	怎	催	崔	吹	客	坑	话	冯	连	法	拍	伟
D	强	纸	床	怎	催	崔	吹	客	坑	话	冯	连	法	拍	伟
E	强	纸	床	怎	催	崔	吹	客	坑	话	冯	连	法	拍	伟
F	强	纸	床	怎	催	崔	吹	客	坑	话	冯	连	法	拍	伟
answer	①	③	④	⑥	②	⑤	④	①	②	⑤	⑥	④	②	①	④
	②	④	①	②	⑤	⑥	③	②	⑤	⑥	①	③	③	②	⑤
	③	⑤	⑥	⑤	④	①	⑥	⑤	⑥	④	④	⑥	④	⑥	③
	④	⑥	②	①	③	④	①	⑥	③	①	③	⑤	①	③	②
	⑤	②	⑤	③	①	③	②	③	④	②	⑤	②	⑤	④	⑥
	⑥	①	③	④	⑥	②	⑤	④	①	③	②	①	⑥	⑤	①

①: AGIS-Net ②: FUNIT ③: DG-Font ④: LF-Font ⑤: MX-Font ⑥: Our FS-Font

Figure 11. User studies on UFSC (unseen font seen character) data. This Figure shows how do we conduct the user study.

content	钚	挫	焦	馁	徉	炜	湮	鲤	狸	滋	揉	扛	怯	姣	迂
reference	去	去	焦	好	得	韩	没	去	去	没	把	差	去	皎	还
	钟	个	你	饭	差	灯	甄	累	累	累	鞣	把	快	好	和
		把		菜				酸	狐	噗					菜
A	钚	挫	焦	馁	徉	炜	湮	鲤	狸	滋	揉	扛	怯	皎	迂
B	钚	挫	焦	馁	徉	炜	湮	鲤	狸	滋	揉	扛	怯	皎	迂
C	钚	挫	焦	馁	徉	炜	湮	鲤	狸	滋	揉	扛	怯	皎	迂
D	钚	挫	焦	馁	徉	炜	湮	鲤	狸	滋	揉	扛	怯	皎	迂
E	钚	挫	焦	馁	徉	炜	湮	鲤	狸	滋	揉	扛	怯	皎	迂
F	钚	挫	焦	馁	徉	炜	湮	鲤	狸	滋	揉	扛	怯	皎	迂
answer	③	⑥	③	④	②	①	④	②	⑥	④	②	⑤	①	⑥	⑤
	②	④	④	⑤	⑤	②	③	③	①	③	⑤	⑥	②	②	⑥
	⑥	①	⑤	③	④	⑥	⑥	④	④	⑥	⑥	④	③	⑤	①
	①	②	⑥	②	③	③	①	①	③	⑤	③	①	⑤	①	④
	④	⑤	②	⑥	①	④	②	⑤	⑤	②	④	②	⑥	③	③
	⑤	③	①	①	⑥	⑤	⑤	⑥	②	①	①	③	④	④	②

①: AGIS-Net ②: FUNIT ③: DG-Font ④: LF-Font ⑤: MX-Font ⑥: Our FS-Font

Figure 12. User studies on UFUC (unseen font unseen character) data. This Figure shows how do we conduct the user study.